GABAergic neurons regulate lateral ventricular development via transcription factor *Pax5*

Nobuhisa Ohtsuka[1,3,*], **Sylvia Badurek**[5,7,*], **Meinrad Busslinger**[6], **Francine M. Benes**[1,3,4,#], **Liliana Minichiello**[5,7,#,&], and **Uwe Rudolph**[2,3,4,#]

[1]Program in Structural and Molecular Neuroscience, McLean Hospital, Belmont, MA, USA
[2]Laboratory of Genetic Neuropharmacology, McLean Hospital, Belmont, MA, USA [3]Department of Psychiatry, Harvard Medical School, Boston, MA, USA [4]Program in Neuroscience, Harvard Medical School, Boston, MA, USA [5]Centre for Neuroregeneration, University of Edinburgh, EH16 4SB Edinburgh, Scotland [6]Research Institute of Molecular Pathology, Vienna Biocenter, Vienna, Austria [7]European Molecular Biology Laboratory, Monterotondo, Italy

Abstract

Postmortem studies have revealed a downregulation of the transcription factor *Pax5* in GABAergic neurons in bipolar disorder, a neurodevelopmental disorder, raising the question whether *Pax5* in GABAergic neurons has a role in normal brain development. In a genetic approach to study functions of *Pax5* in GABAergic neurons, *Pax5* was specifically deleted in GABAergic neurons from *Pax5* floxed mice using a novel *Gad1-Cre* transgenic mouse line expressing Cre recombinase in *Gad1*-positive, i.e. GABAergic neurons. Surprisingly, these mice developed a marked enlargement of the lateral ventricles at approximately seven weeks of age, which was lethal within 1–2 weeks of its appearance. This hydrocephalus phenotype was observed in mice homozygous or heterozygous for the *Pax5* conditional knockout, with a gene dosage-dependent penetrance. By QTL (quantitative trait loci) mapping, a 3.5 Mb segment on mouse chromosome 4 flanked by markers *D4Mit237* and *D4Mit214* containing approximately 92 genes including *Pax5* has previously been linked to differences in lateral ventricular size. Our findings are consistent with *Pax5* being a relevant gene underlying this QTL phenotype and demonstrate that *Pax5* in GABAergic neurons is essential for normal ventricular development.

Keywords

paired box genes; GABA neurons; Gad1-Cre; hydrocephalus

INTRODUCTION

Pax5 is a paired box gene, which functions as a transcription factor in canonical Wnt signaling and determines cellular fate in the cerebral cortex and hippocampus (Machon *et al.*, 2007). In the mid gestation stage, a dynamic gradient of Wnt signaling controls neural tube patterning (Ciani and Salinas, 2005), which is controlled by an organizing center located at the midbrain/hindbrain boundary where *Pax5* is highly expressed (Bouchard *et al.*, 2000). Glutamic acid decarboxylase 67 (GAD_{67}), encoded by the *Gad1* gene, is responsible for synthesis of GABA from glutamate and is widely distributed in the brain (Tamamaki *et al.*, 2003). It is expressed in postmitotic and proliferating cells, suggesting that using this gene promoter to drive Cre will allow recombination of floxed genes at these stages to study fundamental cellular activities such as differentiation and migration during developmental stages (Ma *et al.*, 1992; Tashiro *et al.*, 2007). A *Pax5* global knockout is postnatally lethal (Urbanek *et al.*, 1994). To explore the role of *Pax5* in inhibitory neurons on brain development and function, we have generated GAD_{67}-specific conditional *Pax5*-deficient mice (*Gad1-Pax5*KO).

RESULTS

Generation and analysis of *Gad1-Cre* mice

To achieve expression of the Cre recombinase in GAD_{67}-expressing GABAergic neurons, we generated a *Gad1-Cre* transgenic mouse using chromosomal *Gad1* sequences from a BAC clone (Fig. 1A). *Gad1-Cre* transgenic mice did not show gross abnormalities (Fig. 1B) and were indistinguishable from their wild type (WT) littermates in open-field tests (Fig. S1).

The recombination profile of *Gad1-Cre* transgenic mice was assessed using the reporter lines Rosa26-EYFP (Srinivas *et al.*, 2001) and Z/EG (Novak *et al.*, 2000) in which EYFP (Enhanced Yellow Fluorescent Protein) or EGFP (Enhanced Green Fluorescent Protein) is expressed upon Cre-mediated recombination of a *loxP*-flanked *STOP*-cassette. We observed EYFP-immunoreactive (-IR) cells in various brain areas that contain GABAergic neurons including the brainstem, cerebellum, inferior and superior colliculus, hypothalamus and dentate gyrus of hippocampus and neocortex (mainly layers IV–VI) (Fig. 1B). However, in some brain areas which are rich in GABAergic neurons (Fig. S2) only few cells showed recombination, e.g. in the striatum (Fig. 1B) and the olfactory bulb (data not shown). *Gad1-Cre*-mediated recombination was already present at E12.5 (Fig. 2B) and in P7 pups its pattern was similar to that seen in adult animals (Fig. 2A).

To examine the specificity of recombination events in *Gad1-Cre* mice co-immunostaining studies were performed in the lower layers (layers IV–VI) of the somatosensory cortex. In the mice examined, 100% and 81.8% of EYFP-IR cells were colabeled with GABA, indicating that the recombination is specific for GABAergic cells (Fig. 3A, Table S1, Fig. S4). Conversely, 42.1% and 40.9% of GABA-positive cells were positive for EYFP, indicating that less than half of the GABAergic cells can be targeted by the *Gad1-Cre* recombinase. Some EYFP-IR cells were labeled using an antibody against GAD_{67} (Fig. 3B). However, the GAD_{67} staining is punctated and it is not easy to distinguish signal from background and cell bodies from neurites. We think that this could be the reason why not all EYFP-IR cells are recognized as GAD_{67}-positive. There are multiple populations of GABAergic interneurons, which are defined by the presence of marker proteins. To assess which interneuronal population expresses the *Gad1-Cre* transgene, double-labeling experiments were performed, which revealed that 25.6%–39.8% of the EYFP-positive cells were positive for parvalbumin, and 23.0%–30.9% of parvalbumin-positive cells were colabeled with EYFP (Fig. 3C, TableS1, Fig. S5A). No EYFP-positive cells were co-labeled

with calretinin or neuropeptide Y (TableS1, Fig. S5B). None of EYFP-positive cells was colocalized with the excitatory neurotransmitter glutamate (Fig. 3D, Table S1). Furthermore, *Gad1-Cre*-mediated recombination does not occur in dopaminergic neurons as shown by the absence of reporter signal from tyrosine hydroxylase (TH)-positive neurons (Fig. 3E). Recombination was absent in astrocytes and oligodendrocytes (Fig. 3F,G). Collectively, this initial analysis shows that the *Gad1-Cre* transgene is expressed in parvalbumin-positive interneurons and as yet unidentified interneuron classes, excluding the calretinin or neuropeptide Y-expressing subtypes.

*Gad1-Pax5*KO mice develop hydrocephalus in a gene dosage-dependent manner

The *Gad1-Cre* line was crossed with *Pax5*-floxed mice (Horcher *et al.*, 2001) to generate *Gad1-Pax5*KO mice with a conditional deletion of *Pax5* in GAD_{67}-expressing neurons (Fig. 4A). About 47% of homozygous mutant mice (*Gad1-Cre, Pax5$^{f/f}$*) and 19% of heterozygous mutant mice (*Gad1-Cre, Pax5$^{f/+}$*) developed a dome-shaped skull around postnatal day 50 (Fig. 4B), indicating that the development of hydrocephalus is dependent on the *Pax5* gene dosage (*p=0.0021*, Spearman's rank correlation; Fig. 4C and D). *Gad1-Pax5*KO mice died approximately one to two weeks after the appearance of macroscopic changes (Fig. 4D), and displayed lethargy and emaciation. Both homozygous and heterozygous mutants developing a dome-shaped head had a life expectancy of 58 days (Fig. 4D) whereas animals not developing this phenotype by P60 were able to survive for at least 12 months and were fertile. Abnormalities were not observed in littermates with control genotypes (*Gad1-Cre; Pax5$^{f/+}$; Pax5$^{f/f}$*).

*Gad1-Pax5*KO mice have enlarged lateral ventricles

The ventriculomegaly of *Gad1-Pax5*KO was prominent in the lateral ventricles (Fig. 5, Fig. S6). In the most severe cases, the medial structures between lateral ventricles were deformed and compressed as represented by vertically relocated hippocampi (Fig. 6B, arrow 1). The cerebral cortex surrounding the lateral ventricles was also markedly thinner (Fig. 6B, arrow 2). The ventricular dilation may be caused by obstruction of interventricular connections, increased production of cerebrospinal fluid by ependymal cells of the choroid plexus or decreased resorption by arachnoid villi. Since our present analysis provided no evidence for the enlargement of other ventricles, the extensive enlargement of the lateral ventricles indicates an obstruction of interventricular connections, while other possibilities cannot be excluded. The potential contribution of other mechanisms, e.g. that *Gad1-Cre*-induced recombination in the choroid plexus (Fig. S3) may have affected ependymal cell function, remain to be elucidated.

*Gad1-Pax5*KO mice show increased locomotion and anxiogenic-like behavior in the open field test

Locomotor activity of *Gad1-Pax5*KO mice with dome-shaped heads was assessed in a novel open field. All four measures taken, i.e. distance traveled, speed, time spent in center and number of entries into center showed significant differences in genotype, ($F_{1,77}=20.94$, *p=0.0026*; $F_{1,77}=18.94$, *p=0.0033*; $F_{1,77}=9.1$, *p=0.0196*; $F_{1,77}=9.3$, *p=0.0187*, respectively, by two-way repeated measures ANOVA). Bonferroni posthoc analysis confirmed these differences (Fig. 7A). Since the mutants appeared to be lethargic in their home cages, the increased locomotion is likely induced by the novel environment. The observation that mutant mice spent less time in the center and entered the center less frequently (Fig. 7B, C) is potentially indicating an anxiogenic-like behavior.

DISCUSSION

The major phenotype of these mice, i.e. enlargement of the lateral ventricles has been found to be associated with neurodevelopmental disorders such as schizophrenia (Meduri *et al.*, 2010; Rosa *et al.*, 2010) and bipolar disorder (Kempton *et al.*, 2008) [not in the first episode (Rosa *et al.*, 2010), only when psychosis was present (Edmiston *et al.*, 2011)]. Thus, reduced *Pax5* expression in GABAergic neurons in patients with bipolar disorder (Benes *et al.*, 2007) might contribute to changes of ventricular size observed in these patients.

Pax5 is strongly expressed in the mid-hindbrain boundary (MHB) at embryonic stages while in adults the expression level is low and expression appears to be widespread (Allen Developing Mouse Brain Atlas, http://developingmouse.brain-map.org). It is tempting to speculate that *Pax5*-deficiency in the MHB of the embryo may be responsible for the hydrocephalus phenotype in *Gad1-Pax5*KO mice. However, the time window for the appearance of hydrocephalus is quite narrow, potentially suggesting a role of the *Pax5*-deficit in the adult animals in the pathogenesis of hydrocephalus in the *Gad1-Pax5*KO mice. To address this question, temporal control of *Pax5* expression in GAD_{67}-positive neurons would be required. Our finding that GABAergic neurons can play a role in determining ventricular size is consistent with the observation of a linear correlation between degree of ventricular enlargement and reduction of GAD-immunoreactive neurons in a kaolin-induced hydrocephalus model in rats (Tashiro *et al.*, 1997).

It is interesting to note that one functional copy of Pax5 is not sufficient to maintain a normal development, as a sizable percentage of Gad1-Pax5$^{+/-}$ mice develop hydrocephalus (Fig. 4C). While global Pax5$^{+/-}$ have not been examined in this study, such mice have been generated in other contexts (e.g. as breeders to generate Pax5$^{-/-}$ mice), and development of an obvious hydrocephalus like the one observed in this study has not been noticed, which does not exclude the possibility that a more subtle ventricular enlargement may be present. This raises the question why heterozygous loss of Pax5 in GABAergic neurons leads to hydrocephalus, while global heterozygous loss of Pax5 is so far not known to do so. While we do not know the answer to this question, one speculative possibility is that in global Pax5$^{+/-}$ mice loss of Pax5 in other cell types helps to compensate for loss of Pax5 in GABAergic neurons. Another noteworthy aspect is that not all Gad1-Pax5$^{-/-}$ mice develop hydrocephalus (Fig. 4C), indicating the presence of modifier genes. This is in line with previous observations that several genes have an influence on ventricle size in the mouse (Zygourakis and Rosen, 2003).

Gad1 is thought to be expressed exclusively in neurons, and our analysis supports the notion that the Gad1-Cre transgene is expressed specifically in GABAergic neurons. However, we cannot completely rule out the possibility that Gad1-Cre is also expressed in non-neuronal tissues and that Gad1-Cre-mediated recombination in non-neuronal cells might lead to hydrocephalus. *Gad1* knockout mice (and also *Gabrb3* knockout mice which lack the $GABA_A$ receptor β3 subunit or mice lacking the vesicular inhibitory amino acid transporter *Viaat*) have been found to have a cleft palate phenotype (Asada *et al.*, 1997; Condie *et al.*, 1997; Homanics *et al.*, 1997; Wojcik *et al.*, 2006). The developmental mechanism of cleft palate in these mice are unknown, but it is not unreasonable to assume that non-neuronal cells are involved in the development of cleft palate. However, it has been shown recently that CNS-specific inactivation of *Gad1* was sufficient to disrupt palate development (Oh *et al*, 2010), suggesting that the primary defect is in the CNS. We assume that the same is true for the hydrocephalus phenotype in the Gad1-Pax5$^{-/-}$ mice.

Pax2 and *Pax5* arose by gene duplication and have maintained equivalent biochemical functions (Bouchard *et al.*, 2000). It has been suggested that there is functional substitution

between *Pax2* and *Pax5* in brain regionalization (Schwarz *et al.*, 1997). *Pax2* expression in the MHB positively regulates *Pax5* expression through a Pax-binding site of a minimal MHB-specific enhancer in the 5′-flanking region of *Pax5* (Pfeffer *et al.*, 2000). Combinatorial interactions between the transcription factors *Pax2*, *En1*, *Grg4*, *Otx2*, *Gbx2*, and the signaling molecule *Wnt1* control the expression of *FGF8*, which is required to maintain mid-hindbrain identity by supporting development of multiple neurons (Ciani and Salinas, 2005; Ye *et al.*, 2001). *FGF8*, *Wnt*, *En1*, *En2*, *Pax2* and *Pax5* depend on each other for stable expression; if one is missing, the expression of the remaining genes is extinguished over time, and these genes can induce and maintain each other's expression at ectopic locations (Funahashi *et al.*, 1999; Wurst and Bally-Cuif, 2001; Ye *et al.*, 2001). These interactions establish a positive regulatory loop, which governs brain development as an organizer located at the MHB. The direct interactions between *Pax2* and the MHB-specific enhancer in the 5′-flanking region of *Pax5* mentioned above are directly involved in this feedback loop (Pfeffer *et al.*, 2000). Hydrocephalus has also been observed in other mutants of genes in this regulatory network, e.g. $Otx2^{+/-}$ mice (Makiyama *et al.*, 1997), *Wnt1* null mutants, transgenic mice expressing *En1* ectopically under the control of the *Wnt1* enhancer, and $Wnt1^{sw/sw}$ (*swaying*) point mutants (Louvi and Wassef, 2000; Rowitch *et al.*, 1999; Thomas and Capecchi, 1990), demonstrating the essential role of the MHB region for ventricular development. All previous loss-of-function studies have been performed with global mutants, so that no conclusion could be drawn as to the relevant neuronal cell types required for normal ventricular development. Our data clearly implicate that GABAergic neurons, and in particular, *Pax5*-dependent functions in these neurons, play a pivotal role in this process. The closely related gene, *Pax6*, is expressed in the subcomissural organ (SCO) from which neuroepithelial cells originate, and mice lacking *Pax6* fails to develop the SCO (Estivill-Torrus *et al.*, 2001). In the H-Tx rats which develop congenital hydrocephalus, *Pax6* is downregulated (Miller *et al.*, 2006). Thus, *Pax6* could play a role in the development of hydrocephalus. Recently, it has also been reported that deregulation of the p57-E2F1-p53 axis in the SCO and *Pax2*-positive interneurons results in non-obstructive hydrocephalus and cerebellar malformation in mice (Matsumoto *et al.*, 2011).

QTL mapping revealed a 3.5 Mb locus on chromosome 4 containing 92 genes including *Pax5*, which interacts with another as yet uncharacterized locus on chromosome 7 to modulate ventricle size of the mouse brain (Zygourakis and Rosen, 2003). Our data suggests that *Pax5* is likely a major gene at this locus responsible for modulating ventricle size.

METHODS

Generation of *Gad1-Cre* mouse line

The plasmid pIZKeoX1 containing the *Cre-IRES-lacZ* construct (Fig. 1) was generated in *E. coli*. The *Neo* cassette with flanking *frt* sequences was inserted downstream of the *Cre-IRES-lacZ* in reversed orientation. Homologous arms of 50bp were added for subsequent specific recombination into the first coding ATG of the *Gad1* gene in the BAC clone, RPCI23-118N13 (BACPAC resources, Children's Hospital, Oakland, USA) by ET recombination (Muyrers *et al.*, 2004). Specifically, the cassettes inserted into the BAC clone consists of a hybrid intron (*HI*) followed by the Cre-recombinase encoding gene, an internal ribosomal entry site (*IRES*), the beta-galactosidase gene (*lacZ*) for identification of transgene expression by X-gal staining, and a neomycin/kanamycin cassette (*neo*) for selection of recombined BAC clones in *E. coli*. The *Neo* cassette was removed by Flp-mediated recombination at the *frt* sites after the selection. The consequent transgenic construct was validated also by DNA sequencing at the borders of insertion sites using primer1 5′-ACGGCCGGAGTGGACACCTGTGGAGAG-3′ for the boundary between the first coding ATG of *Gad1* and *Cre*, and primer 2 5′-AGATCAGCAGCCTCTGTTCCACAT

3′ at the boundary between *frt* and *Gad1*. BAC DNA was prepared using a CsCl gradient centrifugation-based method or a QIAGEN kit for large constructs. Circular BAC DNA was injected at 1–2ng/μl into pronuclei of oocytes (CBA/C57 hybrid). Offspring of founder mice was screened for transgene expression by X-gal staining, showing that the *LacZ*-cassette is functional in the cerebellum and superior colliculus (regions with many *Gad1-Cre* and *LacZ* expressing cells). However, *LacZ* expression was relatively weak presumably due to low efficiency of the IRES site. Cre recombinase function was tested in crosses with reporter mice which express EYFP or EGFP after Cre-mediated deletion of a STOP-cassette (Rosa26-EYFP reporter line, Srinivas et al. 2001; *Z/EG* reporter line, Novak et al. 2000).

Generation of *Gad1-Pax5*KO mice

Pax5 floxed mice had been backcrossed to C57BL/6 at least 8 generations, *Gad1-Cre* mice for at least 4 generations. After these backcrossings, *Gad1-Cre* mice were crossed with floxed *Pax5* mice.

Experiments involving mice at the Mailman Research Center of the McLean Hospital were approved by the Institutional Animal Care and Use Committee of McLean Hospital (protocols #07-1/2-1 and #08-1/2-2 to UR), and all animal procedures at the European Biology Molecular Laboratory (Mouse Biology Unit) conformed to National and International laws and policies (EEC Council Directive 86/609, OJ L 358, 1, December 12, 1987; NIH Guide for the Care and Use of Laboratory Animals, NIH Publication No. 85-23, 1985 revised in 1995), personal project number: 7.1; at the Centre for Neuroregeneration, conformed to UK legislation (Scientific procedures) ACT 1986 and the University of Edinburgh ethical review committee policy, personal project license: 60/4049. Mouse reagents will be made available to the research community.

Histology and Immunostainings

Adult mice and pups were anesthetized by intraperitoneal injection of 3% avertin in PBS, and perfused with PBS, followed by 4% PFA in PB buffer (pH7.4) for fixation. Embryos were dissected out of the uterus of the mother (euthanized by cervical dislocation). Dissected brains and embryos were postfixed in 4% PFA at 4 °C overnight, then rinsed twice with cold PBS and stored in cold 30% sucrose in Tris-azide buffer for 2–3 days at 4°C followed by cryopreservation in embedding medium (OCT Sakura TissueTek). Cryosections (30μm) were obtained using a Leica cryostat CM3050S and for DAB stainings were incubated in 0.1M PB buffer (pH7.4), quenched with 2% H_2O_2, washed in TBS, blocked in 10% serum in histo solution (0.3% carrageenan, 0.5% triton X-100, in TBS), incubated with the primary antibody in 1% serum in histo solution at 4°C for 24–72 hrs, washed in wash solution (1% serum in 0.5% triton X-100 in TBS), incubated with the secondary antibody in 1% serum in histo solution at 4°C overnight, rinsed in wash solution, incubated in vectastain ABC solution for 1hr, washed in TBS and TB, and incubated in 0.5mg/ml DAB and 0.03% H_2O_2, followed by cold TB washes, drying and mounting in DEPEC-Eukitt. For immunofluorescent stainings after the primary antibody incubation, sections were washed in TBS and incubated in secondary antibody in TBS at room temperature for 2hrs, washed in TBS, stained with DAPI, dried and mounted in vectashield mounting medium. Stained sections were analyzed using a dissecting microscope (Leica MZ12 and Zeiss Schott KL1500 light source and Leica FireCam 1.2.0 imaging software) or a Leica fluorescent microscope (Leica DMR and camera DC500 and imaging software IM500 or a Leica confocal microscope LASAF TCS SP5). For histological analyses *Gad1-Cre,* and *Pax5* mutant brains were fixed as described above except that animals were anesthetized using Isoflurane and sliced using a coronal brain dice at AP: Bregma +0.38 and −4.16, approximately for macro photography shown in Fig 5 and Fig S6. Series of 25μm coronal

sections were prepared after cryoprotection procedure at 100μm interval, and were subjected to hematoxylin/eosin staining.

Antibodies

EGFP (for DAB:1:2000, ab290 Abcam; for IF:1:3000 ab10980 Abcam), GABA (1:1000, A2052 Sigma), glutamate (1:1000, G9282 Sigma), GAD67 (for DAB: 1:, for IF: 1:1000, MAB5406 Chemicon), parvalbumin (1:1000, P3088 Sigma), calretinin (1:2000, #7699/4 Swant), NPY (1:8000, ab10980 Abcam), TH (1:200, #Mab318 Chemicon), GFAP (1:1000, #sc9065 Santa Cruz), CNPase (1:100, #Mab326 Chemicon), biotinylated anti-chicken, -mouse, -rabbit (1:200, Vector Labs), Alexa488-anti-chicken (1:1000, Molecular Probes), Alexa555-anti-mouse, -rabbit (1:1000, Molecular Probes)

Behavioral Analysis

All behavioral studies were performed on male mice, littermates being housed together. Mice were moved to the behavioral facility at least a week before starting the tests in order to allow for habituation to the new environment.

Novelty-Induced Locomotor Activity in Gad1-Cre Mice

After habituation to the test room four mice at a time were placed into four different open field arenas ($50 \times 50 \times 28$ cm) at light conditions of 100 lux in the arena and video tracked for 30min. The time spent and distance traveled at the border and at the center of the arena were recorded using VideoMot2, version 5.62 (TSE). A 34 cm $\times$ 34 cm square inside the open field was arbitrarily defined as center of the field.

Novelty-Induced Locomotor Activity in *Gad1-Cre Pax5* Mutants

Mice were placed in $42 \times 42 \times 31$ cm plexiglas chambers lit at 160 lux. Mice were videorecorded for 60 minutes. Five minutes time bins were applied to process activity measurements by the aid of computer software EthoVision XT (Noldus Information Technology). A 20 cm $\times$ 20 cm square inside the open field was arbitrarily defined as center of the field.

Statistics

Data in Fig. 4D, "Percent appearance of the symptom" was analyzed by Spearman's rank correlation for number of deleted *Pax5* alleles by appearance of the symptom. Data in Figs. 7 **and** S1 are expressed as mean ± SEM. Data in Fig S1A and B were analyzed by two-way ANOVA (genotype x area). Data in Fig S1C was analyzed by unpaired 2-sample t-test. Data in Fig. 7A,B were analyzed by two-way repeated-measures ANOVA (genotype x time) and the mutant group and control group were compared by two-sided Student's t-test.

Supplementary Material

Refer to Web version on PubMed Central for supplementary material.

Acknowledgments

References

Asada H, Kawamura Y, Maruyama K, Kume H, Ding RG, Kanbara N, Kuzume H, Sanbo M, Yagi T, Obata K. Cleft palate and decreased brain gamma-aminobutyric acid in mice lacking the 67-kDa isoform of glutamic acid decarboxylase. Proceedings of the National Academy of Sciences of the United States of America. 1997; 94:6496–6499. [PubMed: 9177246]

Benes FM, Lim B, Matzilevich D, Walsh JP, Subburaju S, Minns M. Regulation of the GABA cell phenotype in hippocampus of schizophrenics and bipolars. Proc Natl Acad Sci U S A. 2007; 104:10164–10169. [PubMed: 17553960]

Bouchard M, Pfeffer P, Busslinger M. Functional equivalence of the transcription factors Pax2 and Pax5 in mouse development. Development. 2000; 127:3703–3713. [PubMed: 10934015]

Ciani L, Salinas PC. WNTs in the vertebrate nervous system: from patterning to neuronal connectivity. Nat Rev Neurosci. 2005; 6:351–362. [PubMed: 15832199]

Condie BG, Bain G, Gottlieb DI, Capecchi MR. Cleft palate in mice with a targeted mutation in the gamma-aminobutyric acid-producing enzyme glutamic acid decarboxylase 67. Proceedings of the National Academy of Sciences of the United States of America. 1997; 94:11451–11455. [PubMed: 9326630]

Edmiston EE, Wang F, Kalmar JH, Womer FY, Chepenik LG, Pittman B, Gueorguieva R, Hur E, Spencer L, Staib LH, Constable RT, Fulbright RK, Papademetris X, Blumberg HP. Lateral ventricle volume and psychotic features in adolescents and adults with bipolar disorder. Psychiatry Res. 2011; 194:400–402. [PubMed: 22041535]

Estivill-Torrus G, Vitalis T, Fernandez-Llebrez P, Price DJ. The transcription factor Pax6 is required for development of the diencephalic dorsal midline secretory radial glia that form the subcommissural organ. Mech Dev. 2001; 109:215–224. [PubMed: 11731235]

Funahashi J, Okafuji T, Ohuchi H, Noji S, Tanaka H, Nakamura H. Role of Pax-5 in the regulation of a mid-hindbrain organizer's activity. Dev Growth Differ. 1999; 41:59–72. [PubMed: 10445503]

Homanics GE, DeLorey TM, Firestone LL, Quinlan JJ, Handforth A, Harrison NL, Krasowski MD, Rick CE, Korpi ER, Makela R, Brilliant MH, Hagiwara N, Ferguson C, Snyder K, Olsen RW. Mice devoid of gamma-aminobutyrate type A receptor beta3 subunit have epilepsy, cleft palate, and hypersensitive behavior. Proceedings of the National Academy of Sciences of the United States of America. 1997; 94:4143–4148. [PubMed: 9108119]

Horcher M, Souabni A, Busslinger M. Pax5/BSAP maintains the identity of B cells in late B lymphopoiesis. Immunity. 2001; 14:779–790. [PubMed: 11420047]

Kempton MJ, Geddes JR, Ettinger U, Williams SC, Grasby PM. Meta-analysis, database, and meta-regression of 98 structural imaging studies in bipolar disorder. Arch Gen Psychiatry. 2008; 65:1017–1032. [PubMed: 18762588]

Louvi A, Wassef M. Ectopic engrailed 1 expression in the dorsal midline causes cell death, abnormal differentiation of circumventricular organs and errors in axonal pathfinding. Development. 2000; 127:4061–4071. [PubMed: 10952903]

Ma W, Behar T, Maric D, Maric I, Barker JL. Neuroepithelial cells in the rat spinal cord express glutamate decarboxylase immunoreactivity in vivo and in vitro. J Comp Neurol. 1992; 325:257–270. [PubMed: 1460115]

Machon O, Backman M, Machonova O, Kozmik Z, Vacik T, Andersen L, Krauss S. A dynamic gradient of Wnt signaling controls initiation of neurogenesis in the mammalian cortex and cellular specification in the hippocampus. Dev Biol. 2007; 311:223–237. [PubMed: 17916349]

Makiyama Y, Shoji S, Mizusawa H. Hydrocephalus in the Otx2+/- mutant mouse. Exp Neurol. 1997; 148:215–221. [PubMed: 9398463]

Matsumoto A, Susaki E, Onoyama I, Nakayama K, Hoshino M, Nakayama KI. Deregulation of the p57-E2F1-p53 axis results in nonobstructive hydrocephalus and cerebellar malformation in mice. Molecular & Cellular Biology. 2011; 31:4176–4192. [PubMed: 21844226]

Meduri M, Bramanti P, Ielitro G, Favaloro A, Milardi D, Cutroneo G, Muscatello MR, Bruno A, Mico U, Pandolfo G, La Torre D, Vaccarino G, Anastasi G. Morphometrical and morphological analysis of lateral ventricles in schizophrenia patients versus healthy controls. Psychiatry Res. 2010; 183:52–58. [PubMed: 20538436]

Miller JM, Kumar R, McAllister JP 2nd, Krause GS. Gene expression analysis of the development of congenital hydrocephalus in the H-Tx rat. Brain Res. 2006; 1075:36–47. [PubMed: 16469303]

Muyrers JP, Zhang Y, Benes V, Testa G, Rientjes JM, Stewart AF. ET recombination: DNA engineering using homologous recombination in E. coli. Methods Mol Biol. 2004; 256:107–121. [PubMed: 15024163]

Novak A, Guo C, Yang W, Nagy A, Lobe CG. Z/EG, a double reporter mouse line that expresses enhanced green fluorescent protein upon Cre-mediated excision. Genesis. 2000; 28:147–155. [PubMed: 11105057]

Oh WJ, Westmoreland JJ, Summers R, Condie BG. Cleft palate is caused by CNS dysfunction in Gad1 and Viaat knockout mice. PLoS ONE. 2010; 5:e9758. [PubMed: 20333300]

Pfeffer PL, Bouchard M, Busslinger M. Pax2 and homeodomain proteins cooperatively regulate a 435 bp enhancer of the mouse Pax5 gene at the midbrain-hindbrain boundary. Development. 2000; 127:1017–1028. [PubMed: 10662641]

Rosa PG, Schaufelberger MS, Uchida RR, Duran FL, Lappin JM, Menezes PR, Scazufca M, McGuire PK, Murray RM, Busatto GF. Lateral ventricle differences between first-episode schizophrenia and first-episode psychotic bipolar disorder: A population-based morphometric MRI study. World J Biol Psychiatry. 2010; 11:873–887. [PubMed: 20545464]

Rowitch DH, Danielian PS, McMahon AP, Zec N. Cystic malformation of the posterior cerebellar vermis in transgenic mice that ectopically express Engrailed-1, a homeodomain transcription factor. Teratology. 1999; 60:22–28. [PubMed: 10413335]

Schwarz M, Alvarez-Bolado G, Urbanek P, Busslinger M, Gruss P. Conserved biological function between Pax-2 and Pax-5 in midbrain and cerebellum development: evidence from targeted mutations. Proc Natl Acad Sci U S A. 1997; 94:14518–14523. [PubMed: 9405645]

Srinivas S, Watanabe T, Lin CS, William CM, Tanabe Y, Jessell TM, Costantini F. Cre reporter strains produced by targeted insertion of EYFP and ECFP into the ROSA26 locus. BMC Dev Biol. 2001; 1:4. [PubMed: 11299042]

Tamamaki N, Yanagawa Y, Tomioka R, Miyazaki J, Obata K, Kaneko T. Green fluorescent protein expression and colocalization with calretinin, parvalbumin, and somatostatin in the GAD67-GFP knock-in mouse. J Comp Neurol. 2003; 467:60–79. [PubMed: 14574680]

Tashiro Y, Drake JM, Chakrabortty S, Hattori T. Functional injury of cholinergic, GABAergic and dopaminergic systems in the basal ganglia of adult rat with kaolin-induced hydrocephalus. Brain Res. 1997; 770:45–52. [PubMed: 9372201]

Tashiro Y, Yanagawa Y, Obata K, Murakami F. Development and migration of GABAergic neurons in the mouse myelencephalon. J Comp Neurol. 2007; 503:260–269. [PubMed: 17492625]

Thomas KR, Capecchi MR. Targeted disruption of the murine int-1 proto-oncogene resulting in severe abnormalities in midbrain and cerebellar development. Nature. 1990; 346:847–850. [PubMed: 2202907]

Urbanek P, Wang ZQ, Fetka I, Wagner EF, Busslinger M. Complete block of early B cell differentiation and altered patterning of the posterior midbrain in mice lacking Pax5/BSAP. Cell. 1994; 79:901–912. [PubMed: 8001127]

Wojcik SM, Katsurabayashi S, Guillemin I, Friauf E, Rosenmund C, Brose N, Rhee JS. A shared vesicular carrier allows synaptic corelease of GABA and glycine. Neuron. 2006; 50:575–587. [PubMed: 16701208]

Wurst W, Bally-Cuif L. Neural plate patterning: upstream and downstream of the isthmic organizer. Nat Rev Neurosci. 2001; 2:99–108. [PubMed: 11253000]

Ye W, Bouchard M, Stone D, Liu X, Vella F, Lee J, Nakamura H, Ang SL, Busslinger M, Rosenthal A. Distinct regulators control the expression of the mid-hindbrain organizer signal FGF8. Nat Neurosci. 2001; 4:1175–1181. [PubMed: 11704761]

Zygourakis CC, Rosen GD. Quantitative trait loci modulate ventricular size in the mouse brain. J Comp Neurol. 2003; 461:362–369. [PubMed: 12746874]
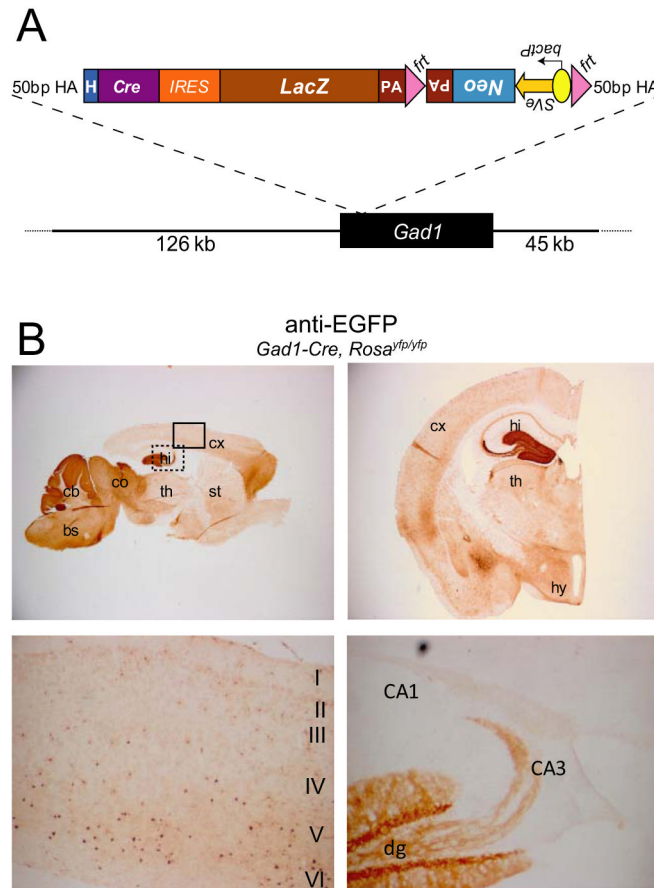
Figure 1. Generation and Characterization of *Gad1-Cre* Transgenic Mice
(**A**) Schematic diagram of the *Cre-IRES-LacZ* transgene that was inserted at the first coding ATG of the *Gad1* gene on BAC RPCI23-118N13. The *Neo* cassette was removed by Flp-mediated recombination at the *frt* sites after selection. (**B**) *Gad1-Cre*-mediated recombination visualized using anti-EG(Y)FP antibody in a 4.5 month-old *Gad1-Cre*, *Rosa26*$^{yfp/yfp}$ mouse. Upper panels: Representative images of a sagittal (left), and a coronal section (right). Lower panels: magnification of the areas indicated with solid and dotted lines in the upper left panel. Lower left panel: layers I–VI of somatosensory cortex. Lower right panel: anterior part of the hippocampus. bs, brainstem; cb, cerebellum; co, colliculi; cx, neocortex; dg, dentate gyrus; hi, hippocampus; hy, hypothalamus; st, striatum; th, thalamus; *bactP*, bacterial promoter; *frt*, Flp recombinase target site; *H*, hybrid intron; HA, homologous arm; *IRES*, internal ribosomal entry site; *LacZ*, beta-galactosidase encoding gene; *Neo*, neomycin resistance gene; *PA*, polyadenylation signal; *SVe*, *SV40* enhancer.
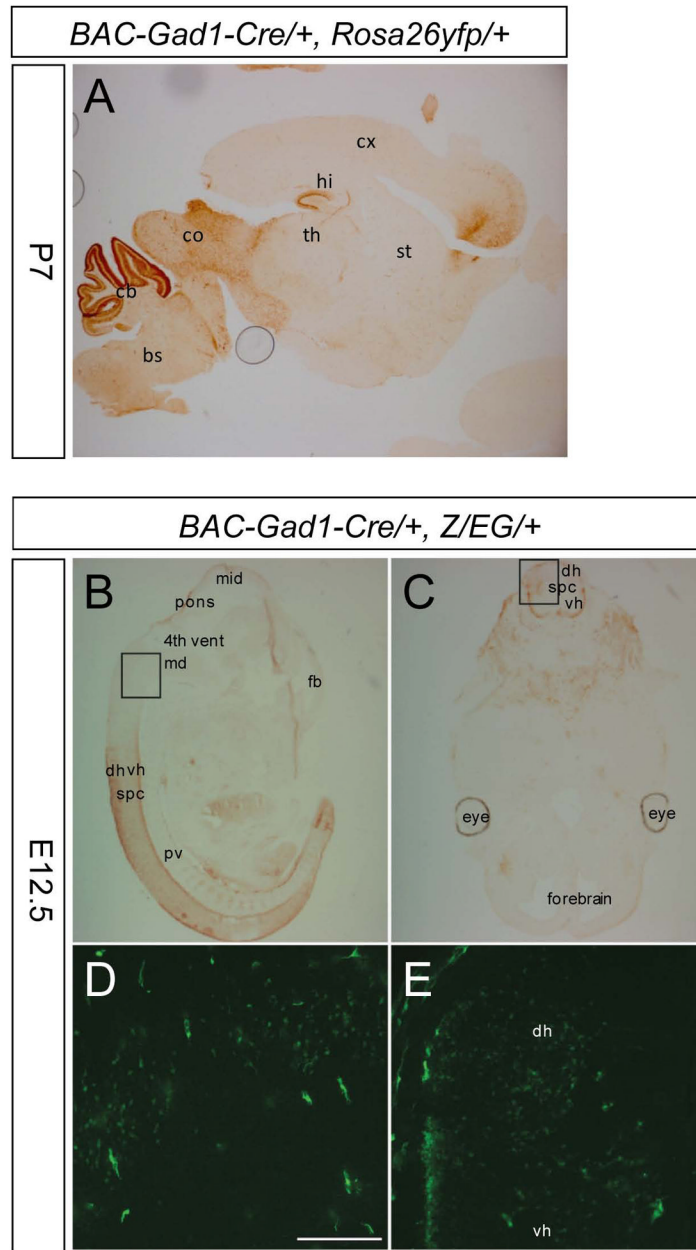
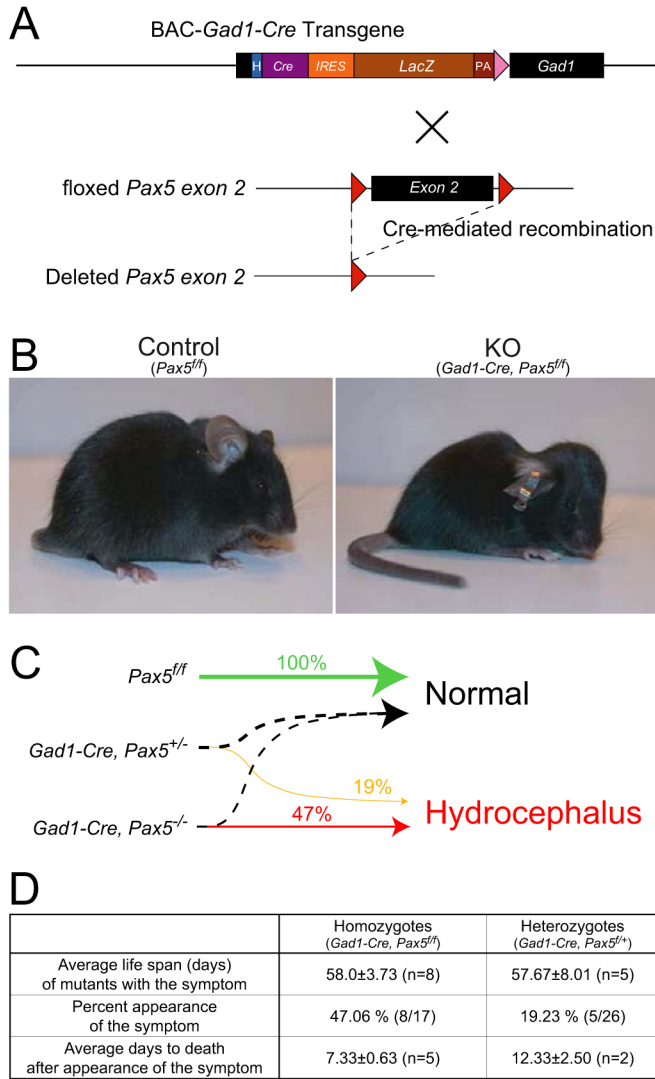**Figure 2. *Gad1-Cre*-Mediated Recombination During Development**
(**A**) Colorimetric immunostaining using an antibody against EG(Y)FP on a sagittal brain section of a P7 *Gad1-Cre, Rosa26*$^{yfp/+}$ mouse. (**B–C**) Colorimetric immunostaining using an antibody against EGFP on a sagittal (**B**) and coronal (**C**) section of an E12.5 *Gad1-Cre, Z/ EG* embryo. (**D–E**) Direct detection of EGFP in *Gad1-Cre, Z/EG* at E12.5. (**D**) Magnified image corresponding to the inset in (B). (**E**) Magnified image corresponding to the inset in (C). bs, brainstem; cb, cerebellum; co, colliculi; cx, neocortex; dh, dorsal horn; fb, forebrain; hi, hippocampus; md, medulla; mid, midbrain; pv, prevertebrae; spc, spinal cord; st, striatum; th, thalamus; vh, ventral horn; 4th vent, 4th ventricle.
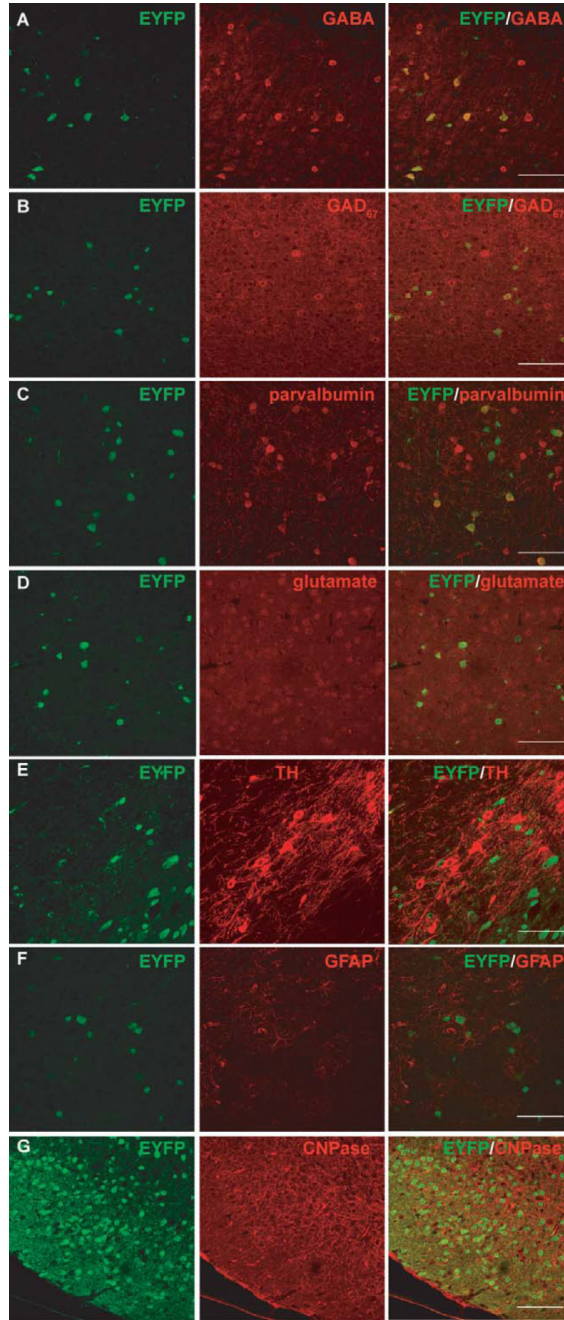
Figure 3. Specific recombination mediated by *Gad1-Cre* in GABAergic neurons but not glutamatergic neurons or glial cells. (A–E)
Double immunostaining of a 4.5 months old *Gad1-Cre, Rosa26$^{yfp/yfp}$* reporter mouse. The recombination marker, EYFP (green) and (**A**) GABA, (**B**) GAD$_{67}$, (**C**) parvalbumin, and (**D**) glutamate (red) were superimposed in the layers IV–VI of somatosensory cortex. (**E**) The recombination marker, EYFP (green) and tyrosine hydroxylase (TH) (red) were superimposed in the substantia nigra. (**F–G**) Double immunostaining of a 3 months old *Gad1-Cre, Rosa26$^{yfp/+}$* reporter mouse. The recombination marker, EYFP (green) and (**F**) glial fibrillary protein (GFAP) (red) in the layers IV–VI of somatosensory cortex and (**G**) 2′,

3′-cyclic nucleotide 3′ phosphodiesterase (CNPase) (red) in the superior colliculus were superimposed. Scale bar: 100μm.

A BAC-*Gad1-Cre* Transgene

floxed *Pax5* exon 2 — Exon 2

Cre-mediated recombination

Deleted *Pax5* exon 2 —

B Control (*Pax5$^{f/f}$*) — KO (*Gad1-Cre, Pax5$^{f/f}$*)

C *Pax5$^{f/f}$* → 100% → Normal

Gad1-Cre, Pax5$^{+/-}$

Gad1-Cre, Pax5$^{-/-}$ → 47% / 19% → Hydrocephalus

D

	Homozygotes (*Gad1-Cre, Pax5$^{f/f}$*)	Heterozygotes (*Gad1-Cre, Pax5$^{f/+}$*)
Average life span (days) of mutants with the symptom	58.0±3.73 (n=8)	57.67±8.01 (n=5)
Percent appearance of the symptom	47.06 % (8/17)	19.23 % (5/26)
Average days to death after appearance of the symptom	7.33±0.63 (n=5)	12.33±2.50 (n=2)

Figure 4. Generation of *Gad1-Pax5*KO and Developmental Phenotype
(**A**) Schematic diagram of generation of the *Gad1-Pax5*KO mice. (**B**) Morphological appearance of a homozygous *Gad1-Cre, Pax5$^{f/f}$* mouse ("KO") characterized by dome-shaped head, kyphosis and emaciation, compared to a *Pax5$^{f/f}$* ("Control") mouse (postnatal days 35, littermates). (**C**) Schematic diagram of gene dosage-dependent partial penetrance of the lateral ventricle dilation of the Gad1-*Pax5*KO (**D**) Life span and prevalence of hydrocephalus in *Gad1-Cre-Pax5*-deficient mice.
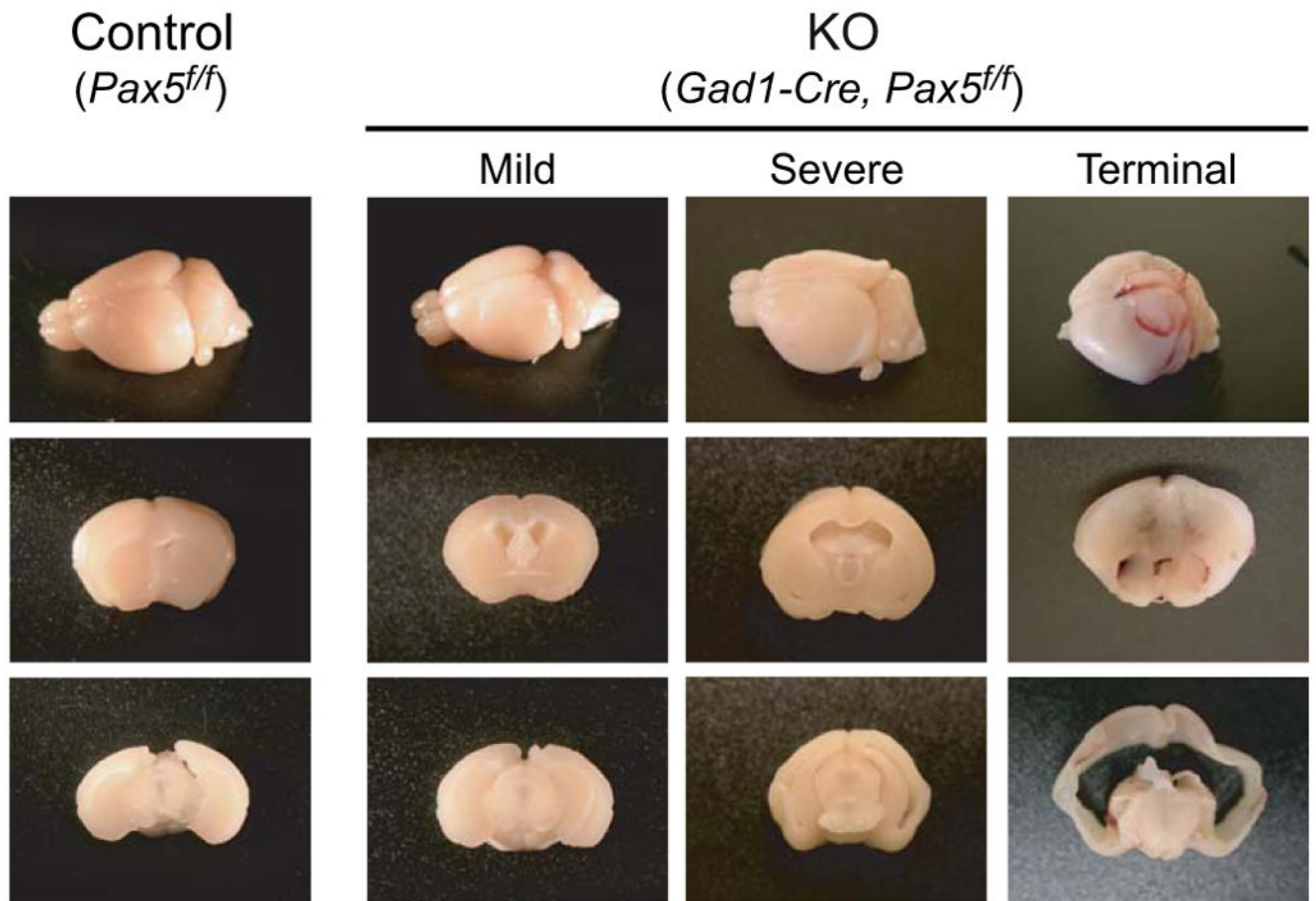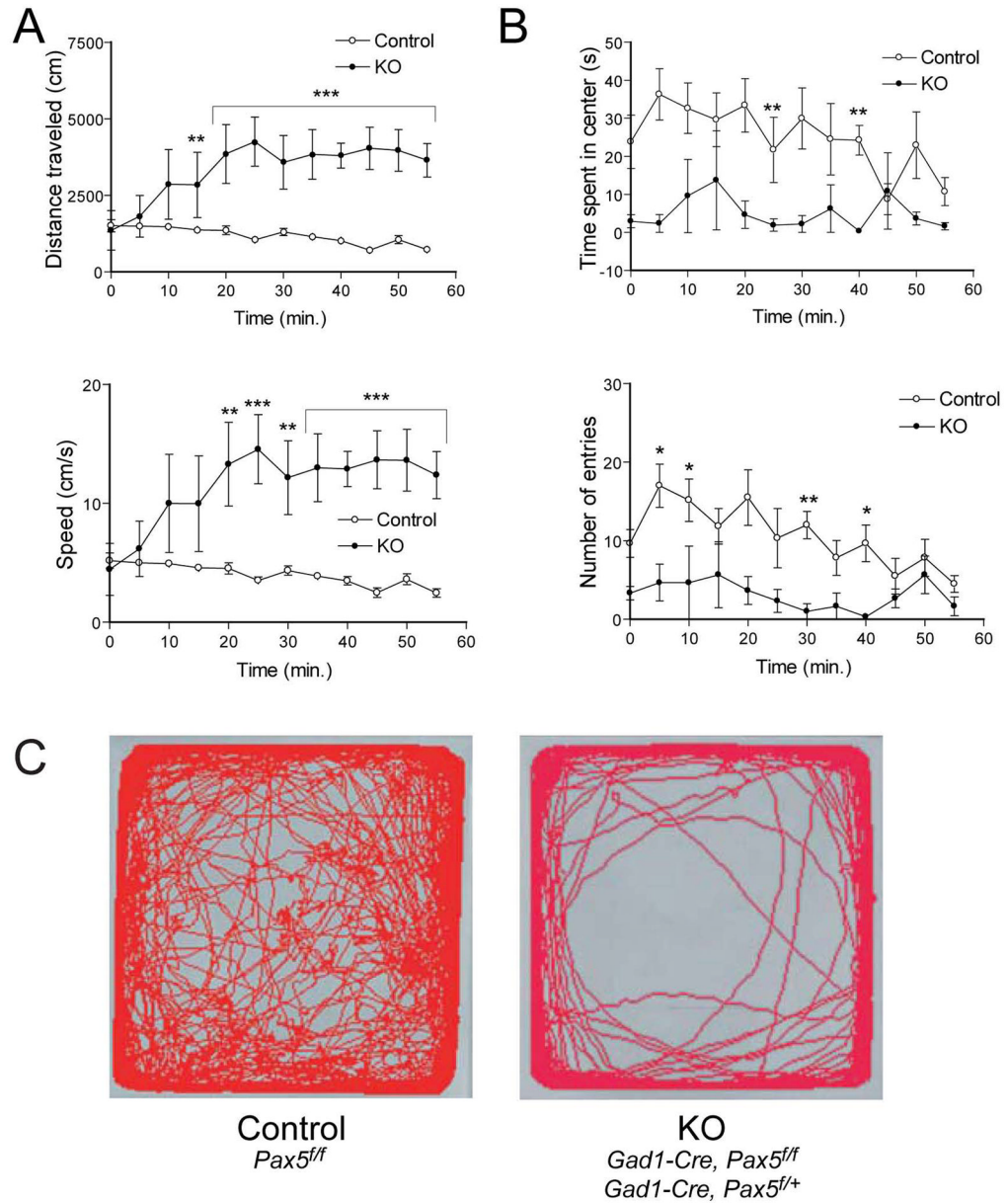
Figure 5. Lateral Ventricle-Specific Dilation in *Gad1-Pax5*KO mice
Brain preparations from three mutant ("KO") mice with examples of either no macroscopic abnormalities ("mild", and "severe", P46) or dome-shaped head ("terminal", P41), and "Control" (P60) mice demonstrating dilation of the lateral ventricles. For further examples, see Fig. S6.
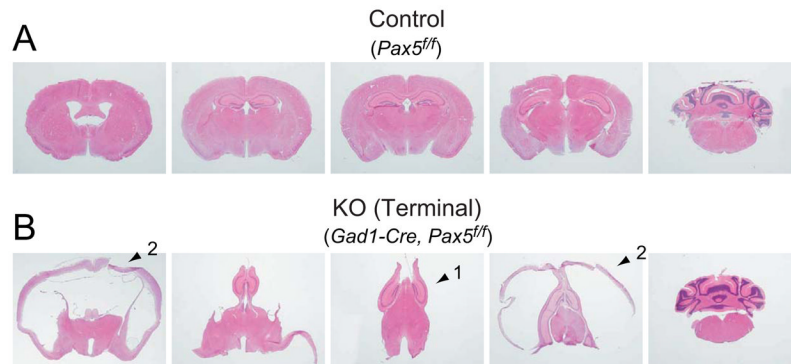
Figure 6. Hematoxylin-eosin staining of coronal serial sections of *Gad1-Pax5*KO mice
Example images of (**A**) "Control" at positions from Bregma: AP-0.34, -1.46, -1.82, -2.46 and -6.36 approximately and (**B**) Sections from equivalent positions from "KO" with dome-shaped head. Postnatal days 60. Arrow 1: hippocampus, arrow 2: cortex.